UKACC International Conference on Control 2012
Cardiff, UK, 3-5 September 2012

Modelling of a Pan and Tilt Servo System

Samuel Sharp and Adam Wicks
Control Systems Department
Chess Dynamics Ltd.
Horsham, United Kingdom
{Samuel.Sharp & Adam.Wicks}@chess-dynamics.com

Andrzej Ordys and Gordana Collier
Faculty of Science, Engineering and Computing
Kingston University
Kingston upon Thames, United Kingdom
{A.Ordys & Gordana.Collier}@kingston.ac.uk

***Abstract*—Two-axis pan and tilt systems are widely used in surveillance applications for high accuracy positioning of sensor payloads such as cameras and laser pointers. In order to develop advanced control algorithms to improve the performance of these systems, a model of the system must be developed. This model should include the dynamics of the system to include effects such as compliance and account for friction effects in the drive. This paper discusses the development of the overall model of the system using National Instruments LabVIEW, and in particular, the models for friction and the drive train that will be used.**

Keywords-Servo systems; Modelling; Software tools; Harmonic drives

I. INTRODUCTION

Chess Dynamics Ltd. is a supplier of high performance Radar and Electro-Optic systems for the defence industry. It designs and manufactures precision two-axis pan & tilt camera systems for land, naval and airborne applications.

The performance demands of these systems are very high; requiring high pointing resolution and high positional accuracy with fast tracking speeds and smooth low speed control.

Research and development is being conducted within the company through a Knowledge Transfer Partnership (KTP) scheme with Kingston University to develop advanced control methods that will improve the accuracy and tracking performance of the company's products.

Initially, simulation models of the system will be developed to allow advanced control and estimation algorithms to be evaluated and tested before being implemented into the actual system. Subsequent stages of the project will develop estimation algorithms to improve the quality of sensor measurements and then control algorithms will be developed and evaluated as to their suitability for increasing system performance.

This paper discusses the models of the system that have been developed and their implementation in National Instruments' LabVIEW software using the Control Design and Simulation toolkit.

Finally, simulation results are compared to results obtained from a representative experimental test rig.

II. SYSTEM MODELLING

In this section, we will begin by introducing the system to be modelled before going on to discuss the models for the individual components of the system. Finally, the implementation of the overall system model in different forms using LabVIEW is discussed.

A. System Overview

The system to be modelled, shown in Figure 1, is a compact two-axis pan and tilt system designed to carry an optical sensor payload of up to 25kg.

Figure 1 - Cobra Product [1]

The system consists of two identical drive assemblies, with integrated encoders, mounted on the azimuth and elevation axes. Housed within the body of the system are two current-mode servo amplifiers to drive each axis and the main control board to interface to the amplifiers and the outside world via a

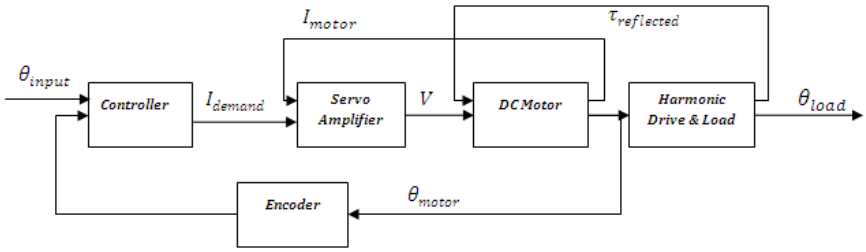

Figure 2 - Single Axis Servo System Control Block Diagram

serial interface. The software on this board implements the digital controller that controls the position and rate of the platform.

Initial investigations will consider a single axis only as the dynamics of each axis will be similar due to having the same drive components and electronics. It also provides a simplified system that can be easily tested and used for validating the models. It is, however, understood that the azimuth and elevation dynamics are not independent (for example, the azimuth inertial load will change as the elevation axis rotates).

The overall block diagram showing the feedback relationships between the main components of the system for a single axis is shown in Figure 2.

The details of modelling the components of the servo system from the servo amplifier to the load will now be discussed.

B. Servo Amplifier

The servo amplifier used is a current-mode linear DC amplifier capable of providing up to 2A of current. The DC relationship was found by experimentation and connecting the amplifier to a large resistive load and measuring the current across it. This provided information on the DC Gain but did not give any information about higher frequency dynamics.

The experiment was conducted using LabVIEW, a CompactRIO and a Fluke 8808a Digital Multimeter (DMM) as shown in Figure 3. The 8808a DMM was connected to the CompactRIO via the serial interface, using plug and play instrument drivers to configure and read the current measurements. Meanwhile, the CompactRIO fed an analogue voltage to drive the servo amplifier across its full range.

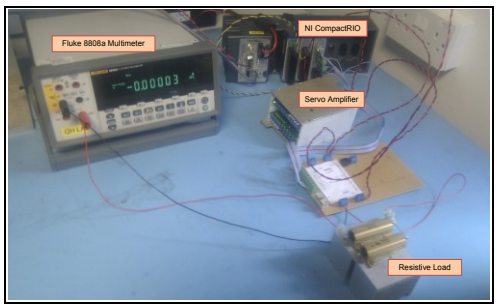

Figure 3 - Servo Amplifier Characterisation Experiment Setup

The servo amplifier was modelled as a proportional current feedback loop with a voltage saturation to represent the maximum voltage supply that can be supplied to the motor.

C. DC Motor

The DC Motor used in the system is a high performance brushed DC motor. The motor is modelled as a two-input (voltage and load torque) and single output (motor shaft velocity) system. The DC motor model consists of two sub-processes, an electrical and mechanical, as detailed in [1].

The electrical sub-process is described by Equation 1, where I_a is the armature current, U_a is the armature voltage, L_a is the armature inductance, R_a is the armature resistance, ω is the angular velocity and Ψ represents the magnetic flux.

$$I_a(t) = \frac{1}{L_a}\int_0^t \big(U_a(t) - R_a I_a(t) - \Psi\omega(t)\big)\mathrm{dt} + \mathrm{I_a}(0) \quad (1)$$

The mechanical process is described by Equation 2, where J is the inertia of the motor, K_t is the motor torque constant from the electrical sub-process, M_l is the load torque and M_f is the friction torque in the motor.

$$\omega(\mathrm{t}) = \frac{1}{J}\int_0^t (K_t I_a - M_l - M_\mathrm{f})\mathrm{dt} + \omega(0) \quad (2)$$

D. Harmonic Drive

The gearing used in the system is a harmonic drive, or strain wave gear, developed in the 1950's for the aerospace industry. It is a compact, lightweight gearbox with high gear ratios and zero backlash. Disadvantages of this type of gearing include high static friction, nonlinear compliance and high flexibility. Considerable research has been conducted into the modelling, friction compensation and control of harmonic drives due to their favourable transmission attributes [3][4][5].

From the research conducted in this field, a number of different models have been proposed for harmonic drive gears. Some of these models will now be discussed.

1) Hashimoto & Kiyosawa

The dynamic model proposed in [6] considers two primary nonlinear effects of harmonic drives, Coulomb friction (τ_f) and a linear stiffening spring (K). The dynamic equations for the model are shown by Equation 3.

$$\begin{aligned} J_l\ddot{\theta}_l - K\left(\frac{\theta_m}{N} - \theta_l\right) &= 0 \\ NJ_m\ddot{\theta}_m + K\left(\frac{\theta_m}{N} - \theta_l\right) + N\tau_f &= N\tau_m \\ \tau_l &= K\left(\frac{\theta_m}{N} - \theta_l\right) \end{aligned} \quad (3)$$

2) Ghorbel & Gandhi

The models proposed in [7] and [8] are significantly more complex and take into account additional nonlinear effects and more advanced friction models. The model, represented by τ_{fr} and shown in Equation 4, uses a LuGre friction model that takes into account Stribeck, Dahl, viscous and Coulomb friction effects and an additional position dependent component. Kinematic error in the harmonic drive is represented by $\tilde{\theta}_p$ as a function of the motor position and an additional damping term, caused by the stiffness in the drive, is represented by B_{sp}.

$$J_m\ddot{\theta}_m + K\left(\theta_l - \frac{\theta_m}{N} + \tilde{\theta}_p\right)\left[-\frac{1}{N} + \frac{d\tilde{\theta}_p}{d\theta_m}\right] + B_{sp}\left(\dot{\theta}_l - \frac{\dot{\theta_m}}{N} + \dot{\tilde{\theta}}_p\right)\left[-\frac{1}{N} + \frac{d\tilde{\theta}_p}{d\theta_m}\right] + \tau_{fr} = \tau_m \quad (4)$$

$$J_l\ddot{\theta}_l + K\left(\theta_l - \frac{\theta_m}{N} + \tilde{\theta}_p\right) + B_l\dot{\theta}_l + B_{sp}\left(\dot{\theta}_l - \frac{\dot{\theta_m}}{N} + \dot{\tilde{\theta}}_p\right) = 0$$

3) Ghorbel & Dhaouadi

The model suggested in [9] uses a nonlinear function, represented by $\tau(\dot{\theta}, \theta)$, to model a nonlinear torsional spring with nonlinear viscous damping and a function τ_f to represent a dry friction torque that includes the static friction, as shown in Equation 5.

$$J_m\ddot{\theta}_m + B_m\dot{\theta}_m + \tau_f + \frac{\tau(\dot{\theta}, \theta)}{N} = \tau_m$$
$$J_l\ddot{\theta}_l + B_l\dot{\theta}_l + \tau_l - \tau(\dot{\theta}, \theta) = 0 \quad (5)$$
$$\tau(\dot{\theta}, \theta) = g^{-1}\left[\frac{\dot{\theta}}{h(\theta)}\right] + f(\theta)$$
$$\theta = \frac{\theta_m}{N} - \theta_l$$

4) Taghirad

A more in-depth analysis of the friction effects in harmonic drives are proposed in [3]. The frictional components of the wave generator bearing (τ_{f1}), gear meshing (τ_{f2}) and output bearing are all considered separately in a friction model comprising velocity-dependant Coulomb, viscous and Stribeck friction. T_{meas} represents the compliance model between the motor and load side positions. In comparison to the other models discussed, the motor and load inertias are considered as an overall effective inertia, J_{eff}. The overall model of the harmonic drive was therefore as per Equation 6.

$$K_m i - \frac{1}{N}(T_{meas}) = J_{eff}\ddot{\theta}_{wg} + (\tau_{fm} + \tau_{f1} + \tau_{f2}) \quad (6)$$

5) Tjahjowidodo, Al-Bender & Van Brussel

The work carried out in [10] proposed a model for the torsional compliance of the harmonic drive and then performed identification on the drives in two test setups using a low and high-torque class of harmonic drive. The harmonic drive model was then described by Equation 7, with equations for the input (motor) side and load side dynamics.

$$J_m\ddot{\theta}_m + \frac{\left[T_b(\Delta\tilde{\theta}) + T_h\left(\Delta\tilde{\theta}, \Delta\dot{\tilde{\theta}}\right)\right]}{N+1} = \tau_m$$
$$J_l\ddot{\theta}_l + T_h\left(\Delta\tilde{\theta}, \Delta\dot{\tilde{\theta}}\right) + T_f(\Delta\theta_l, \Delta\theta_l) = 0 \quad (7)$$

In Equation 7, $\tilde{\theta}$ is the difference between the motor and load angles, T_b is a third order polynomial function to represent a nonlinear spring, T_h represents the torsional stiffness and T_f is the bearing friction torque of the harmonic drive.

E. Overall System Model

This section deals with the different representations of the overall system model built from the components previously discussed and their implementation in LabVIEW.

The initial model of the system developed encompassed the models of the DC motor and servo amplifier discussed and the harmonic drive model detailed in Section 1) of II.D. It consists of a load inertia and a linear spring to represent the compliance between the motor and load side angles. Friction in the system was considered for each of the motor and harmonic drive separately as a linear damping function. The initial overall model of the mechanical system is shown in Figure 5.

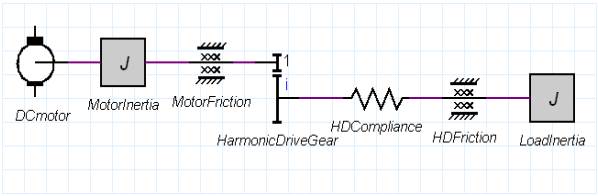

Figure 5 - Overall System Model Diagram

1) Simulation Model

Firstly, a simulation model was developed to represent the system from the dynamical equations as discussed previously. This simulation model was implemented in LabVIEW using the Control Design and Simulation toolkit as shown in Figure

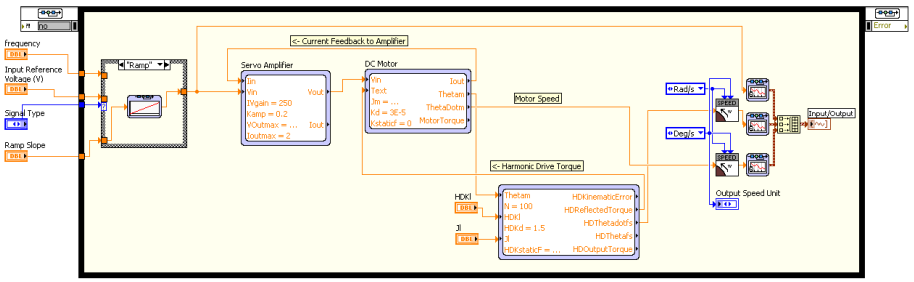

Figure 4 - Simulation Model of System in LabVIEW

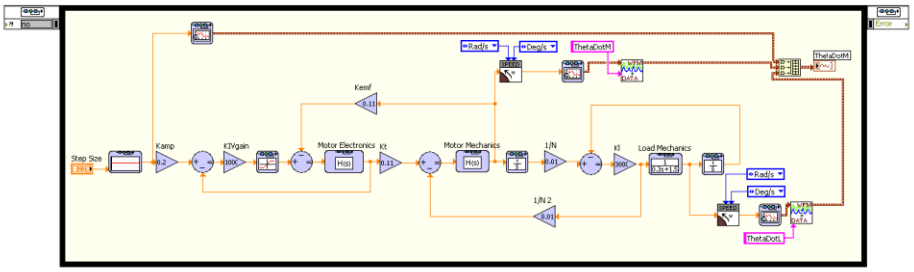

Figure 6 - Transfer Function Representation

4.

2) Transfer Function Model

Having a transfer function representation of the system is important to allow the use of classical design and analysis tools. From the system models, a transfer function representation using the Laplace transform was developed and implemented in LabVIEW, as shown in Figure 6.

3) State Space Model

The need for a state space model of the system allows for the use of modern control design and analysis tools and estimation algorithms such as the Kalman Filter rely on a state-space model of the system. They are also more suited to multiple-input multiple-output (MIMO) systems.

The state space model was implemented in LabVIEW using a MathScript node, allowing the state space equations, parameters and state space model to be defined in a textual way, as shown in Figure 7.

III. Simulation Results

To test the correct operation of the model, simulations were run with a range of input signals. Known parameters of the system were used along with values for unknown parameters that demonstrate the operation of the model. Responses of the system to a step and sinusoidal input for the transfer function model are shown in Figure 8 and Figure 10.

Experiments were carried out for a small number of input signals to an experimental test rig containing a drive assembly of the type being modelled connected to a representative inertia for the Cobra product (including payload). This test rig will be used to validate the models and then controllers developed in the simulation will be verified using the physical test rig.

The results of running the experiments for the same input signals as shown in Figure 8 and Figure 10 are shown in Figure 9 and Figure 11.

The linear model proposed in this paper does not take into account the most important non-linear characteristic of the harmonic drive unit, the high static friction. This is shown by the discontinuity around the zero-output crossing point of the sine response, as shown in Figure 11. Current work is looking to include this effect in a future iteration of the model.

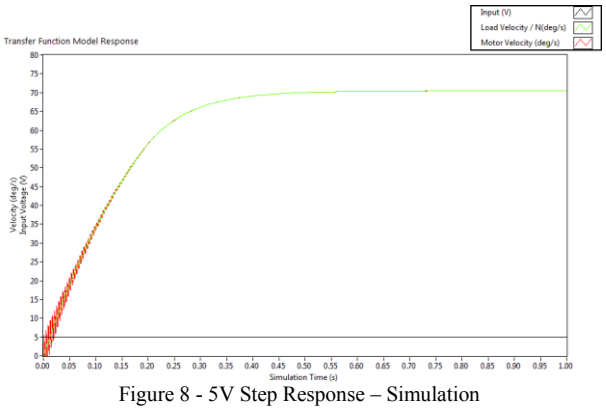

Figure 8 - 5V Step Response – Simulation

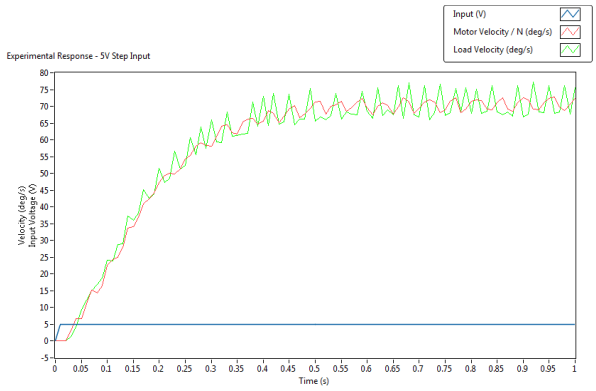

Figure 9 - 5V Step Response – Experiment

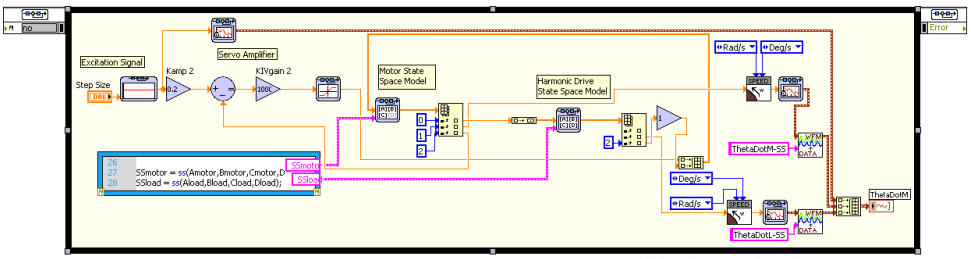

Figure 7 - State Space Representation of System Model using MathScript

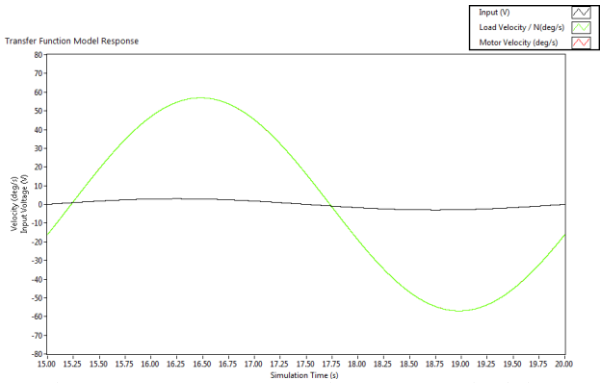

Figure 10 - 3V Low-Frequency Sine Response - Simulation

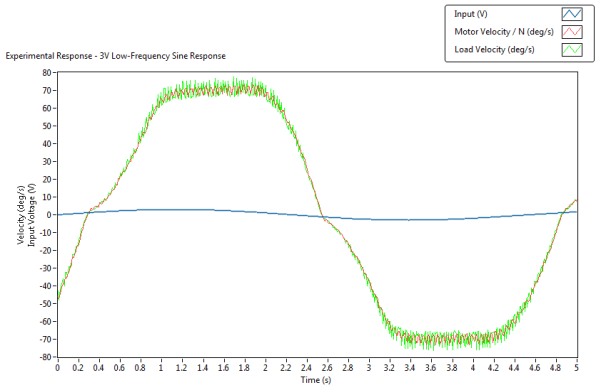

Figure 11 - 3V Low-Frequency Sine Response – Experiment

Comparing the results of the simulation and experiment, the general response of the simulation is similar, however, the experimental results exhibit measurement noise due to the quantisation error in the quadrature encoder. Also, in the experimental sine response, the maximum velocity is reached during the cycle and this limit is not reached in the simulation, as shown by the smooth sine response in Figure 10.

IV. Further Work

Now that a model of the system has been developed and implemented using LabVIEW, further work will look at validating the model to ensure that it reflects the physical system being modelled. This will be conducted on the experimental test rig to provide a known system with which to test the system. The models can then be enhanced to include further dynamical effects and also to evaluate some of the other harmonic drive models discussed previously.

The initial model included only linear friction models, but it will be possible to extend the model to evaluate some of the nonlinear friction models that incorporate additional effects such as static and Coulomb friction, as surveyed in [11]. One example is the positional dependent friction as discussed in [8]. It was confirmed that this exists within the experimental test rig; this will be quantified and added to a future iteration of the model.

Within the larger scope of the full KTP project, the models developed will be used to test and evaluate control and estimation algorithms to evaluate the potential benefits in terms of increased performance of Chess Dynamics' products.

V. Conclusions

In this paper, a model for a two axis servo platform has been introduced. Firstly, an outline of the system was presented, followed by models for the individual components of the system with the main area of interest being the harmonic drive gear system.

The overall model of the system was then presented and different representations of the model were then derived (simulation, transfer function and state space).

Results of running the simulation for various input signals were shown and the model was shown to lack one of the key nonlinearities of the physical system which has the most significant impact on its performance. The simulation results were then compared to the results from the physical test rig using the same input signals.

Finally, the direction of further work in the area was discussed as part of the overall KTP project.

References

[1] Chess Dynamics Ltd. Cobra product [Image]. 2012.

[2] D. Vrancic, D. Juricic, T. Hofling. Measurements and mathematical modeling of a DC motor for the purpose of fault diagnosis, University of Ljubljana. Rep. DP-7091. 1994.

[3] H. Taghirad and P. Bélanger. An experimental study on modelling and identification of harmonic drive systems, in *Proc. 35th Conf. Decision and Control*, 1996, pp. 4725-30.

[4] J. P. Hauschild, G. Heppler and J. McPhee. Friction compensation of harmonic drive actuators, in *Proc. 6th Int. Conf. Dynamics and Control of Systems and Structures in Space*, Italy, 2004, pp. 683-692.

[5] R. Dhaoudi. Torque control in harmonic drives with nonlinear dynamic friction compensation. *Journal of Robotics and Mechatronics*, Vol. 16, No. 4, pp. 388-389, 2004.

[6] M. Hashimoto, Y. Kiyosawa. Experimental study on torque control using harmonic drive built-in torque sensors. *Journal of Robotic Systems*, Vol. 15, No. 8, pp. 435-445, 1998.

[7] F. Ghorbel and P. Gandhi. On the kinematic error in harmonic drive gears, in *Journal of Mechanical Design Trans. ASME*, Vol. 123, pp. 90-97, 2001.

[8] P. Gandhi, F. Ghorbel, J. Dabney. Modelling, identification and compensation of friction in harmonic drives, in *Proc. 41st IEEE Conf. Decision and Control,* 2002, pp. 160-166.

[9] R. Dhaouadi and F. Ghorbel. Modelling and analysis of nonlinear stiffness, hysteresis and friction in harmonic drive gears. *Int. Journal Modelling and Simulation,* Vol. 28, No. 3, pp. 329-336, 2008.

[10] T. Tjahjowidodo, F. Al-Bender and H. Van Brussel. Nonlinear modelling and identification of torsional behaviour in harmonic drives, in *Proc. ISMA,* 2006, pp. 2785-2796.

[11] B. Armstrong-Helouvry, P. Dupont and C. Canudas de Wit. A survey of models, analysis tools and compensation methods for the control of machines with friction. *Automatica,* Vol. 30, No. 7, pp. 1083-1138, 1994.